ACS OMEGA

http://pubs.acs.org/journal/acsodf

Article

Development of a Method for Fast Assessment of Protein Solubility Based on Ultrasonic Dispersion and Differential Centrifugation Technology

Dongwei Wei, Meng Wang, Hongdi Wang, Guijin Liu, Jun Fang,* and Yanbin Jiang*

Cite This: *ACS Omega* 2022, 7, 31338−31347

Read Online

ACCESS | Metrics & More | Article Recommendations | Supporting Information

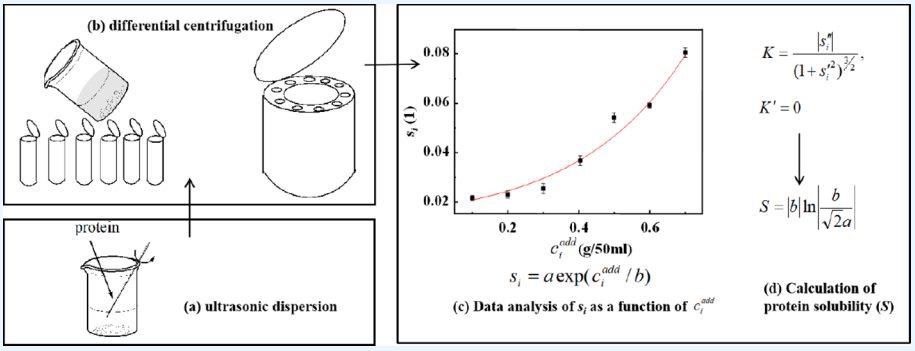

ABSTRACT: Protein solubility is very important for protein crystallization, bioprocess development, and protein application. In this study, a method based on the stability of a protein dispersion system is proposed for fast assessment of protein solubility, which mainly involves ultrasonic dispersion, differential centrifugation, and spectral measurement (UDDCS) and curvature estimation. The appropriate ultrasonic time and centrifugal time were experimentally determined at first. The results show that the relationship between the standard deviation and the protein concentrations originally added accords with the modified exponential equation, and the corresponding concentration of the maximum curvature point is defined as the solubility of the protein. Lysozyme solubility data in NaCl aqueous solutions and zein solubility data in ethanol aqueous solutions are selected to verify the UDDCS method by comparing the data obtained by the UDDCS method and the results from references, and the results indicate that the UDDCS method is reliable, universal, and time-saving. Finally, measurements of zein solubility in NaOH solution and casein solubility in urea aqueous solution were conducted as test cases by the UDDCS method.

HIGHLIGHTS

- A method based on the stability of a protein dispersion system for a general evaluation of protein solubility is proposed.
- Ultrasonic dispersion and differential centrifugation technologies are utilized in the method.
- A modified exponential equation, its curvature equation, and the maximum curvature are selected to analyze the experimental data and determine the protein solubility.
- The method is verified by data from the literature and tested by case studies.

1. INTRODUCTION

Protein solubility, defined as the concentration of soluble protein, is very significant in protein crystallization, bioprocess development, and protein application.[1−3] In protein crystallization, the bottleneck of the three-dimensional structural analysis of protein molecules is the crystallization of suitable high-quality crystals. Protein solubility is one of the most important parameters to study the crystallization process, and it is particularly important to determine the driving force for nucleation and growth processes.[4−6] In bioprocess development, the knowledge of protein solubility under various conditions is one of the most essential data needed for a directed process development. The process steps in the biotechnological purification sector where knowledge of protein solubility is absolutely crucial comprise controlled protein precipitation,[7,8] chromatography,[9,10] aqueous two-phase systems (ATPS), and protein formulation.[11−15] In protein applications, protein solubility is a major issue in many fields,

Received: June 14, 2022
Accepted: August 10, 2022
Published: August 22, 2022

including high-throughput structural genomics,[16,17] human diseases,[18] and industrial applications.[19−21]

When determining solubility data for the development of the processes mentioned above, one has to distinguish between the requirement of thermodynamically sound data and "rough" estimates on regions where spontaneous precipitation/aggregation might occur.[22] Therefore, the methods for measuring protein solubility presented in the literature can be divided into those aiming at determining the thermodynamic solubility and the kinetically controlled precipitation. The thermodynamic solubility curve can be determined very precisely nowadays and is crucial for a scientific thermodynamic approach. Nevertheless, it is also characterized by a need for protein crystals before starting the experiment, sophisticated instrumentation, and relatively long experimental timelines. Although, for most processes, the biotechnology industry only requires data on spontaneous precipitation and kinetic effects in the time frame of hours to days, the protein solubility curve based on the kinetically controlled precipitation still lacks precise solubility determination.[22] A considerable amount of methods describing ways to determine protein solubility can be found in the literature. The methods based on the thermodynamic solubility include equilibrium methods,[23−27] microcolumn techniques,[28−31] the scintillation method,[32,33] several interferometry methods,[34−38] the spin filter method,[39] the artificial neural network method,[40,41] and so on. Usually, establishing a solubility curve of protein is time-consuming[42−45] mainly because the precipitation or the growth rate of protein crystals is much slower than that of small molecules.[23,42]

This study focuses on a method based on ultrasonic dispersion, differential centrifugation, and spectral technology (namely, UDDCS), which aims at fast assessment of protein solubility with reasonable reliability. A modified exponential equation, its curvature equation, and the maximum curvature are selected to analyze the experimental data and determine the protein solubility. Previously published methods and their results are selected to verify the UDDCS method, and zein and casein are selected as the model proteins to test the UDDCS method.

2. FUNDAMENTAL OF THE UDDCS METHOD

The UDDCS method is proposed based on the principle of protein dissolution, which is introduced first as follows.

2.1. Base Principle of Protein Dissolution. The principle of protein dissolution is explained by the protein dissolution two-step theory and a protein/precipitant phase diagram.

According to the theory of dry protein dissolved in solvents of Van Oss,[46] most dried proteins are not immediately soluble in solvents, but they do become solvent-soluble if they are capable of being strongly solvated. In other words, solubility of dry proteins is a two-step procedure, that is, step 1: solvation and step 2: solubilization. It must be assumed that in step 1, the tertiary configuration of the peptide chains, upon solvation, reassumes its native position in which the more solvophilic moieties become oriented outward. Once a sufficient degree of solvation is achieved, the solvated proteins become completely soluble in solvents (step 2), which was proved by Li et al.[47] in that the primary reason could be explained as solvent protonation.

Based on the theories mentioned above, Figure 1 shows the protein/precipitant phase diagram,[48] which indicates that the protein/precipitant phase diagram is divided into four zones by three curves with the concentration increase of protein

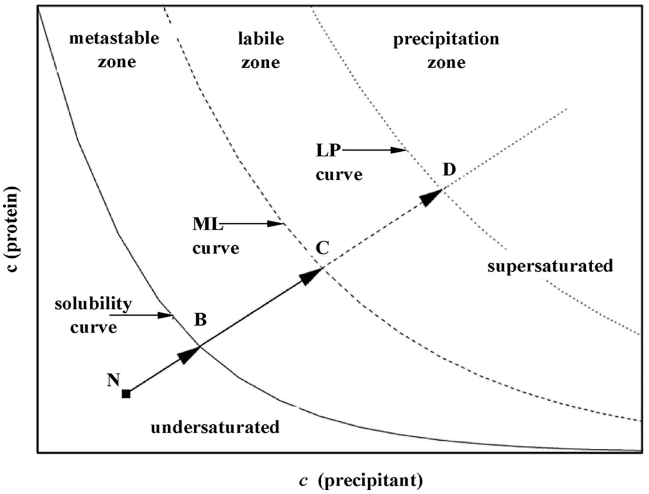

Figure 1. Schematic illustration of the concentrations for an arbitrary system via solvent evaporation or protein addition in a protein/precipitant phase diagram.

dispersions. The three curves are the solubility curve, the ML curve between the metastable and labile zone, and the LP curve between the labile and precipitation zone, respectively. The four zones are the undersaturated zone, metastable zone, labile zone, and precipitation zone, and the latter three zones belong to the supersaturated zone.

When solvent evaporation has occurred or more protein is added to an arbitrary protein dispersion system located in the undersaturated zone, as it is at point N in Figure 1, the protein concentration increases and the thermodynamic solubility curve is crossed (point B). In the undersaturated zone, according to the two-step theory, the protein dispersion system is completely solvated and dissolved where the system is stable. However, in the metastable zone, the solvation degree of protein molecules decreases and so does the stability of the dispersed system. Nevertheless, unless the solution is seeded by a crystal or crystallization is initiated by other means, no crystals will form in the metastable zone. With a continuingly concentrating sample concentration, the labile zone is reached at point C. At point C, the system stability deteriorates dramatically from the metastable zone to the labile zone because concentrating the solution further means that spontaneous nucleation can occur. Thus, in the labile zone, the solvation degree of protein molecules further decreases, and so does the stability of the system. In the precipitation zone, the protein will form amorphous aggregates where the stability of the system is the worst. Meanwhile, the reports on the time needed to establish equilibrium in the supersaturated region suggest that the rate of solvent evaporation is too rapid to determine the "thermodynamic" solubility.[24,29,48] Thus, it can be assumed that the phase transition curve measured represents the transition to a region where spontaneous precipitation or aggregation occurs.[22]

In short, protein dissolution includes dispersion, solvation, and solubilization. The stability of an arbitrary protein dispersion system deteriorates along with increasing concentrations of the protein dispersion. At the ML curve containing point C, the rate of stability deterioration of the dispersion is the fastest because, in the metastable zone, no crystals form; however, in the labile zone, spontaneous nucleation occurs.

2.2. Proposal for the UDDCS Method. When developing the UDDCS method, we focus on the stability of the protein dispersion or solution, and the "solubility curve" obtained is the

https://doi.org/10.1021/acsomega.2c03666
ACS Omega 2022, 7, 31338−31347

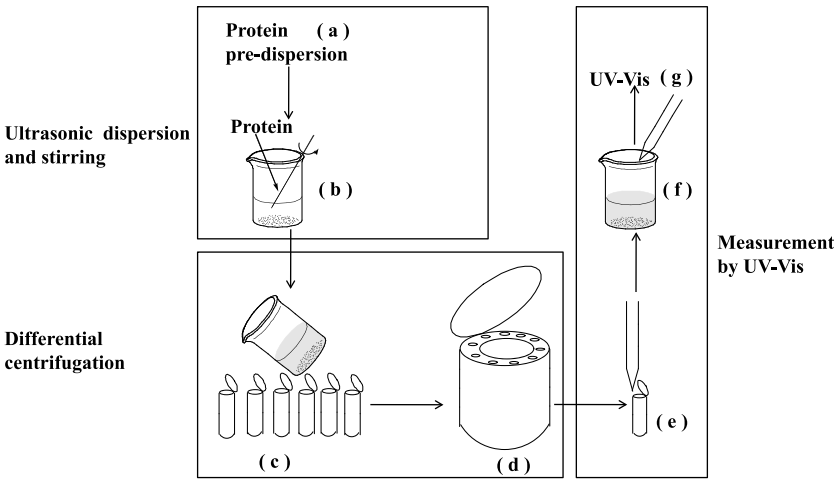

Figure 2. Schematic overview of the experimental procedure: (a, b) ultrasonic dispersion and stirring, (c, d) differential centrifugation, and (e–g) measurement by UV–vis.

ML curve in Figure 1. To obtain the "solubility curve", three important problems should be taken into account: (1) how to make protein disperse and dissolve fast and completely, (2) how to evaluate the stability of the protein dispersion, (3) and based on analysis of the stability of the protein dispersion, how to evaluate the solubility of the protein.

To solve the three problems mentioned above, first, ultrasonic and stirring dispersion are utilized to obtain the protein dispersion system, which is desperately dispersed in a short time. When the protein is added to a solvent and dispersed using ultrasonic and stirring, it will be quickly dispersed into small particles, and a colloid dispersion system will soon be established. The inner solvophilic moieties of protein molecules will be outstretched and soon solvated. Thus, the system can be dispersed completely and approaches the dissolution equilibrium in a short time.

Second, the stability of a protein dispersion system can be evaluated by the variation of supernatant concentrations at different centrifugal speeds because the dispersed but not dissolved protein particles should be separated at a certain centrifugal speed. The greater the variation, the less stable the protein dispersion system is, and the extent of variation can be expressed by calculating the standard deviation (s_i) of supernatant concentrations at different centrifugal speeds. Thus, in the UDDCS method, differential centrifugation technology is utilized to evaluate the stability of the protein dispersion.

Third, according to the principle of protein dissolution mentioned above, the stability of the protein dispersion deteriorates along with the addition of the protein in a certain solvent. At the ML curve in Figure 1, the stability of the protein dispersion shows the fastest deterioration. Therefore, if the s_i of a series of protein concentrations originally added (c_i^{add}) is calculated in terms of the second step, the relationship between s_i and c_i^{add} can be correlated, and the curvature equation of the fitted curve should have a maximum curvature value. The c_i^{add} corresponding to the maximum curvature value, that is, the ML curve shown the in Figure 1, is defined as the "protein solubility" in the UDDCS method. Experimental results show that the relationship between s_i and c_i^{add} accords with the modified exponential equation.

3. MATERIALS AND METHODS

3.1. Materials. Zein was purchased from Sigma-Aldrich Shanghai Trading Co. Ltd. (food grade quality, China). Lysozyme (Ly) and casein (Cas) were purchased from the Shanghai Yuanye Bio-Technology Co., Ltd. (biological reagent, China). NaCl, NaOH, tetramethylsilane (TMS), ethanol (Et), dimethylsulfoxide (DMSO), and urea were purchased from the Guangdong Guanghua Sci-Tech Co., Ltd. (AR, China). Water used in the experiment was deionized water.

3.2. Experimental Procedure, Apparatus, and Data Analysis. The apparatus and experimental procedure of the UDDCS method is illustrated in Figure 2, which contains three procedures, that is, ultrasonic dispersion and stirring, differential centrifugation, and measurement by a UV–vis spectrometer. Procedure a of Figure 2 shows that, before measuring the protein solubility, pre-dispersion is required to be carried out for evaluating the approximate range of protein solubility. At room temperature, protein is gradually added to a certain solvent and ultrasonically dispersed by stirring thoroughly until it forms a protein dispersion with obvious precipitation. Therefore, the approximate protein solubility is obtained. As shown in procedure b of Figure 2, according to the pre-dispersion result, proteins with equal quality intervals (m_i) are added to a certain number of beakers (i) containing the same volume of solvent (v) and ultrasonically dispersed with stirring thoroughly until forming a protein dispersion with a certain c_i^{add}, where c_i^{add} is calculated by eq S1. Procedures c and d of Figure 2 illustrate that each protein dispersion mentioned above is evenly decanted into several centrifugal tubes (n) and centrifuged at different speeds of j_n (rpm). The centrifugal tubes with different c_i^{add} values are centrifuged together at the same centrifugal speed. After centrifugation, the centrifugate supernatant ($c_i^{j_n}$) is removed (procedure e of Figure 2), diluted (procedure f of Figure 2), and measured by use of a UV–vis spectrometer (procedure g of Figure 2). Triple tests were run in parallel. To directly indicate the relationship of the parameters mentioned above, the arrangement for data analysis of the UDDCS method is listed in Table 1.

3.2.1. Appropriate Ultrasonic Time. All samples were dispersed at a constant ultrasonic strength of 40 kHz and 200 W, and the ultrasonic time can be determined by testing the supernatant concentration of protein dispersions as a function of ultrasonic time. For example, at ambient temperature, eight

https://doi.org/10.1021/acsomega.2c03666
ACS Omega 2022, 7, 31338–31347

Table 1. Arrangement for Data Analysis of the UDDCS Method

	$c_i^{j_n}$(g/L)						
	j_n (rpm)						
c_i^{add} (g/L)	j_1	j_2	j_3	j_4	j_5	...	s_i
c_1^{add}	$c_1^{j_1}$	$c_1^{j_2}$	$c_1^{j_3}$	$c_1^{j_4}$	$c_1^{j_5}$	...	s_1
c_2^{add}	$c_2^{j_1}$	$c_2^{j_2}$	$c_2^{j_3}$	$c_2^{j_4}$	$c_2^{j_5}$	...	s_2
c_3^{add}	$c_3^{j_1}$	$c_3^{j_2}$	$c_3^{j_3}$	$c_3^{j_4}$	$c_3^{j_5}$		s_3
c_4^{add}	$c_4^{j_1}$	$c_4^{j_2}$	$c_4^{j_3}$	$c_4^{j_4}$	$c_4^{j_5}$	...	s_4
c_5^{add}	$c_5^{j_1}$	$c_5^{j_2}$	$c_5^{j_3}$	$c_5^{j_4}$	$c_5^{j_5}$	...	s_5
c_6^{add}	$c_6^{j_1}$	$c_6^{j_2}$	$c_6^{j_3}$	$c_6^{j_4}$	$c_6^{j_5}$	...	s_6
c_7^{add}	$c_7^{j_1}$	$c_7^{j_2}$	$c_7^{j_3}$	$c_7^{j_4}$	$c_7^{j_5}$	...	s_7
c_8^{add}	$c_8^{j_1}$	$c_8^{j_2}$	$c_8^{j_3}$	$c_8^{j_4}$	$c_8^{j_5}$	...	s_8
c_9^{add}	$c_9^{j_1}$	$c_9^{j_2}$	$c_9^{j_3}$	$c_9^{j_4}$	$c_9^{j_5}$	...	s_9
...	...	...	...	...	...	...	...

protein dispersions were prepared, and for each dispersion, 1 g of zein weighed by an analytical balance (AL104, Mettler Toledo, Switzerland) was added to 50 mL of 8 g/L NaOH aqueous solutions and dispersed by stirring at a speed of 300 rpm by a stirrer (MS-M-S10, Dragon-Lab, China) for 10 min until without visible aggregations then treated by ultrasonic (KQ5200B, Kunshan Ultrasonic Instrument Co. Ltd., China) for 0, 20, 40, 60, 90, 120, 180, and 240 s. The dispersions are stirred at a speed of 300 rpm for 5 min again and allowed to settle for 20 or 40 min. A volume of 1 mL of the supernatant is sampled and diluted to measure the concentration.

3.2.2. Appropriate Centrifugal Time. The appropriate centrifugal time is determined according to the relationship between the supernatant concentrations and centrifugal time. For example, when the temperature was maintained at 25 °C in a thermostatic bath (THTD-2008W, NingBo Tianheng Instrument Factory, China), 0.6, 1.0, 1.4, and 1.8 g of zein were added to 50 mL of 8 g/L NaOH aqueous solution and ultrasonically dissolved thoroughly with stirring at a speed of 500 rpm. Then, the dispersions were evenly decanted into n centrifugal tubes and centrifuged at a speed of 500 rpm by a centrifugal machine (TDL-80-2B, Shanghai Right Instrument Co., Ltd., China). The centrifugal time was set as 0, 5, 10, 15, 20, and 25 min, respectively. After centrifugation, 0.4 mL of the supernatant was removed from each centrifugal tube and diluted with 7.6 mL of deionized water. The protein concentrations of diluted solutions were tested using UV−vis spectroscopy, and the appropriate centrifugal time is selected when the protein concentration become stable. Triple tests were run in parallel.

In this study, n is set as 6 and centrifugal speeds (j_n) are set as 500, 1000, 1500, 2000, 2500, and 3000 rpm individually.

3.2.3. Measurement of the Protein Concentration. The standard curves of the absorbance (A) and protein concentrations in the dilute protein dispersion ($c_{protein}$) are established as follows. An amount of 0.01, 0.02, 0.03, 0.04, 0.05, 0.06, 0.07, 0.08, 0.09, and 0.1 g of the protein are added to 10 beakers containing 50 mL of solvent individually; then, the dispersion systems are ultrasonically dispersed at room temperature stirring at a speed of 300 rpm to form a dilute solution. The protein can be dissolved completely under these conditions. The absorbance of each solution mentioned above is measured by use of a UV−vis spectrometer (UV-2450, SHIMADZU, Japan) to obtain the standard curve.

A series of different c_i^{add} values of the protein are centrifuged by differential centrifugation according to Table 1. The supernatant is removed after differential centrifugation and diluted with solvent. Then, $c_i^{j_n}$is tested by a UV−vis spectrometer.

As shown in Figure 2, procedures a and b are used to obtain the approximate protein solubility, and c and d are used to get the supernatant of the protein solution through differential centrifugation, and the concentration is measured by UV−vis (procedures e, f, and g). The s_i of the protein solution at different centrifugal speeds with same c_i^{add} values is calculated, and when the protein is added, a series of s_i values can be obtained. Therefore, the equation of s_i as a function of c_i^{add} can be fitted as an exponential equation, and the c_i^{add} corresponding to the maximum curvature value of the equation is defined as the "protein solubility" in the UDDCS method.

3.2.4. Data Analysis. Table 1 shows the arrangement for data analysis of the UDDCS method, c_i^{add}, j_n, and $c_i^{j_n}$, are listed and the standard deviation of each row is calculated. s_i is calculated by eq S6, where $\overline{c_i^{j_n}}$ is the mean value of $c_i^{j_n}$, $\overline{c_i^{j_n}} = \sum_{n=1}^{n} \frac{c_i^{j_n}}{n}$.

According to the principle of the UDDCS method mentioned above, the tendency of s_i from top to bottom should increase, that is, $s_1 < s_2 < s_3 ... < s_8 < s_9 ... < s_i$, which follows the modified exponential equation; therefore, eq 1 is adopted to correlate s_i and c_i^{add}.

$$s_i = a\exp(c_i^{add}/b) \tag{1}$$

where a and b are the amplitude and decay constants of the modified exponential function, respectively.

The maximum curvature point of eq 1 is calculated as follows. The curvature equation of eq 1 can be expressed as eq S7,[49] where K is the curvature, s_i' and s_i'' are the first and second derivatives of eq S7, respectively. Since eq S7 has a maximum curvature point, there is a numeric to make the first derivative of eq S8 equal to zero. The first derivative of eq S8 is obtained from eq S9. If $K' = 0$, eq S10 is obtained.

Therefore, the corresponding concentration at the maximum curvature point, where the rate of stability deterioration is fastest, can be obtained by eq 2 and determined as the solubility of the protein (S).

$$S = |b|\ln\left|\frac{b}{\sqrt{2}\,a}\right| \tag{2}$$

3.3. Verification and Test Studies. *3.3.1. Verification.* Ly solubility in NaCl aqueous solutions were measured by Berg et al.[43] in which a high-throughput method was utilized and by Forsythe et al.[50] where a microcolumn technology was used. The zein solubility in Et aqueous solutions was measured by Evans et al.[51] based on measuring the zein "critical peptization temperature". The UDDCS method was verified by comparing the solubility data of Ly and zein measured by the UDDCS method with the data mentioned above.

Ly solubility in 50 mL of 0.15, 0.3, 0.4, 0.5, 0.6, and 0.8 M NaCl aqueous solutions was measured by the UDDCS method at 18 °C and pH 6.5. Measurement of each $c_i^{j_n}$was repeated in triplicate.

The zein solubility in Et aqueous solutions with different Et:H_2O (w/w) ratios, namely, 11.4:1, 10.76:1, 10.1:1, 9.46:1, 8.8:1, 8.15:1, and 7.5:1, was measured using the UDDCS method at 20 °C, where the mass of H_2O was 3 g for each experiment.

3.3.2. Test Studies. For further illustrating the feasibility of the UDDCS method, the solubility of zein in NaOH aqueous solutions and Cas in urea aqueous solutions was evaluated by the

https://doi.org/10.1021/acsomega.2c03666
ACS Omega 2022, 7, 31338−31347

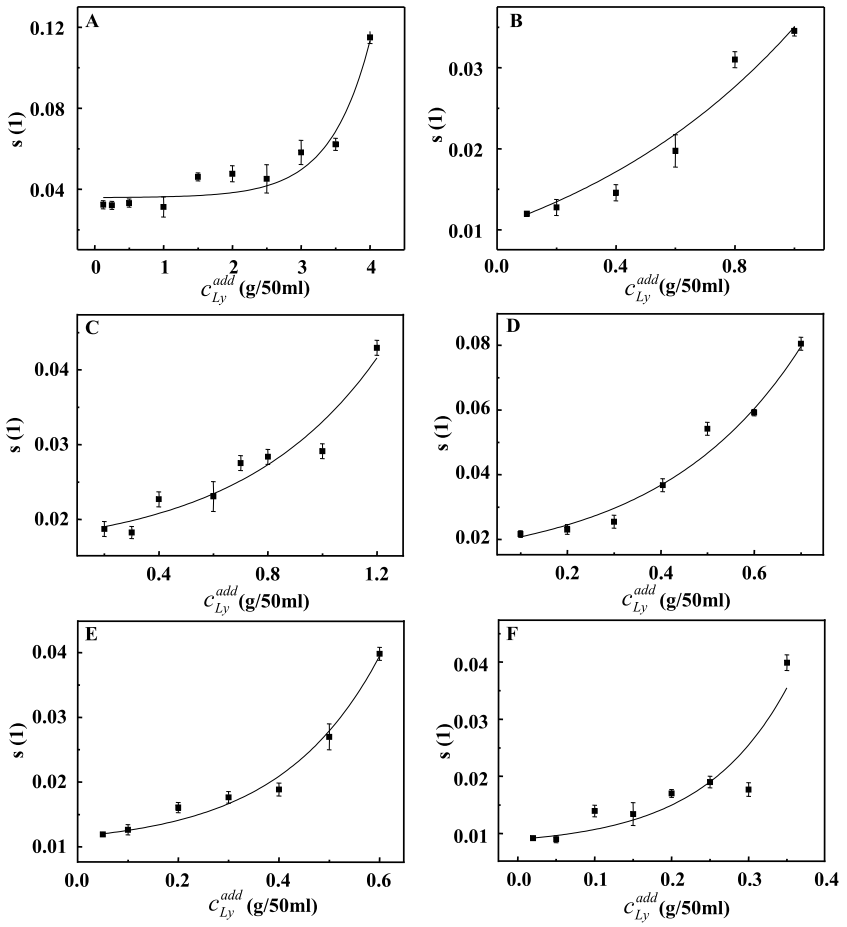

Figure 3. Relationship between s_i and c_{Ly}^{add} at 18 °C, pH 6.5. (A) 0.15 M, (B) 0.3 M, (C) 0.4 M, (D) 0.5 M, (E) 0.6 M, and (F) 0.8 M NaCl aqueous solutions.

UDDCS method. Measurement of each c_i^{in} was repeated in triplicate.

To determine the zein solubility in NaOH aqueous solutions at 20 °C in 50 mL of NaOH aqueous solution, experiments were carried out and c_{NaOH} was set as 2, 4, 6, 8, 10, and 12 g/L. ^{1}H NMR spectra were recorded on a Bruker spectrometer (Bruker AV600, Bruker Co., Switzerland) to investigate the effect of c_{NaOH} on the zein solubility too where zein was dissolved in deuterated DMSO, and all chemical shifts were reported in the parts per million downfield from TMS.

For the effect of temperature on the zein solubility in NaOH aqueous solutions, experiments were carried out using 50 mL of 6 g/L NaOH aqueous solution at 10, 20, 30, 40, 50, and 60 °C.

While measuring the Cas solubility in urea solution, 0, 2, 4, 6, 8, and 10 g of urea were added to 50 mL of H_2O for increasing the solubility, 0.1 g of NaOH was also added to each solution.

4. RESULTS AND DISCUSSION

4.1. Determination of Ultrasonic Time, Centrifugal Time, and Protein Standard Curves. Figure S1 shows the relationship between the supernatant concentration of the protein dispersion and ultrasonic time, and the error bars represent the standard deviation. Figure S1 indicates that the supernatant concentration of protein dispersion reached a balance after ultrasonics for 40 s. Thus, 40 s of ultrasonic time is selected as the feasible ultrasonic time in this study.

Figure S2 indicates that, despite the protein concentration, the supernatant concentration become stable when the centrifugal time is approximately 10 min, and if the centrifugal speed increases, the centrifugal time will shorten. Thus 10 min is sufficient and selected as the proper centrifugal time.

In this study, Ly, zein, and Cas were selected as the model proteins, and the results of standard curve equations of Ly in NaCl aqueous solution, zein in Et/H_2O and NaOH aqueous solution, and Cas in urea aqueous solution are shown in eqs S2−S5, respectively.

4.2. Verification of the UDDCS Method. *4.2.1. Ly Solubility in NaCl Aqueous Solutions.* Figure 3 demonstrates that s_i rises with the increase of c_{Ly}^{add}, and all the fitted curves correlated with eq 1 accord well with the exponential growth. The fitting parameters of a, b, and R^2 of the fitting equations in Figure 3 are listed in Table S1, and the value of R^2 suggests that eq 1 can be successfully used to correlate s_i and c_{Ly}^{add}.

The fitting parameters of equations in Table S1 are substituted into eq 2, and the Ly solubility data in different c_{NaCl} values are obtained and shown in Figure 4. It indicates that S_{Ly} decreases along with the increase of c_{NaCl} and reaches a low limit. Compared with Ly solubility data measured by Berg et al.[43] and Forsythe et al.[50] under the same conditions, Figure 4 indicates that the solubility curve measured by the UDDCS method is located in the middle of the other two curves.

The differences among the three solubility curves of Ly under the same conditions can be explained by the principles of the three methods. The principle of measuring the Ly solubility by a high-throughput method in Berg et al.'s work[43] is to observe whether the precipitation occurs. The principle of microcolumn

https://doi.org/10.1021/acsomega.2c03666
ACS Omega 2022, 7, 31338−31347

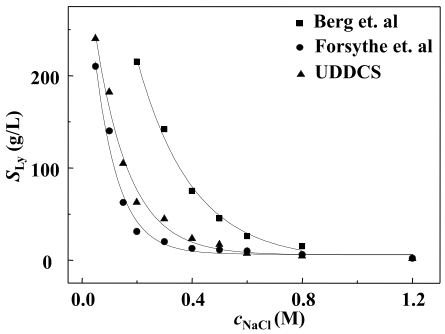

Figure 4. Comparison of Ly solubility data measured by different methods.

technology in Forsythe et al.'s work[50] is to make the protein solution reach the thermodynamic equilibrium as far as possible. According to the principle of the UDDCS method, the protein solubility curve is measured based on the stability of protein dispersions. Therefore, the Ly solubility curve of Berg et al.[43] in Figure 4 basically is the LP curve containing point D in Figure 1, the solubility curve of Forsythe et al.[50] basically is the solubility curve containing point B in Figure 1, and the "solubility curve" measured by the UDDCS method is basically the ML curve containing point C in Figure 1. The result completely accords with the original design of the UDDCS method.

4.2.2. Zein Solubility in Et Aqueous Solution. Figure 5 shows the relationship between s_i and c_{zein}^{add} in different Et:H_2O (w/w) solutions at 20 °C, and the fitting parameters of a, b, and R^2 of the fitting equations are listed in Table S2, which indicates that eq 1 can be successfully used to correlate s_i and c_{zein}^{add}.

The fitting parameters are substituted into eq 2, and zein solubility data in different Et:H_2O (w/w) solutions are obtained

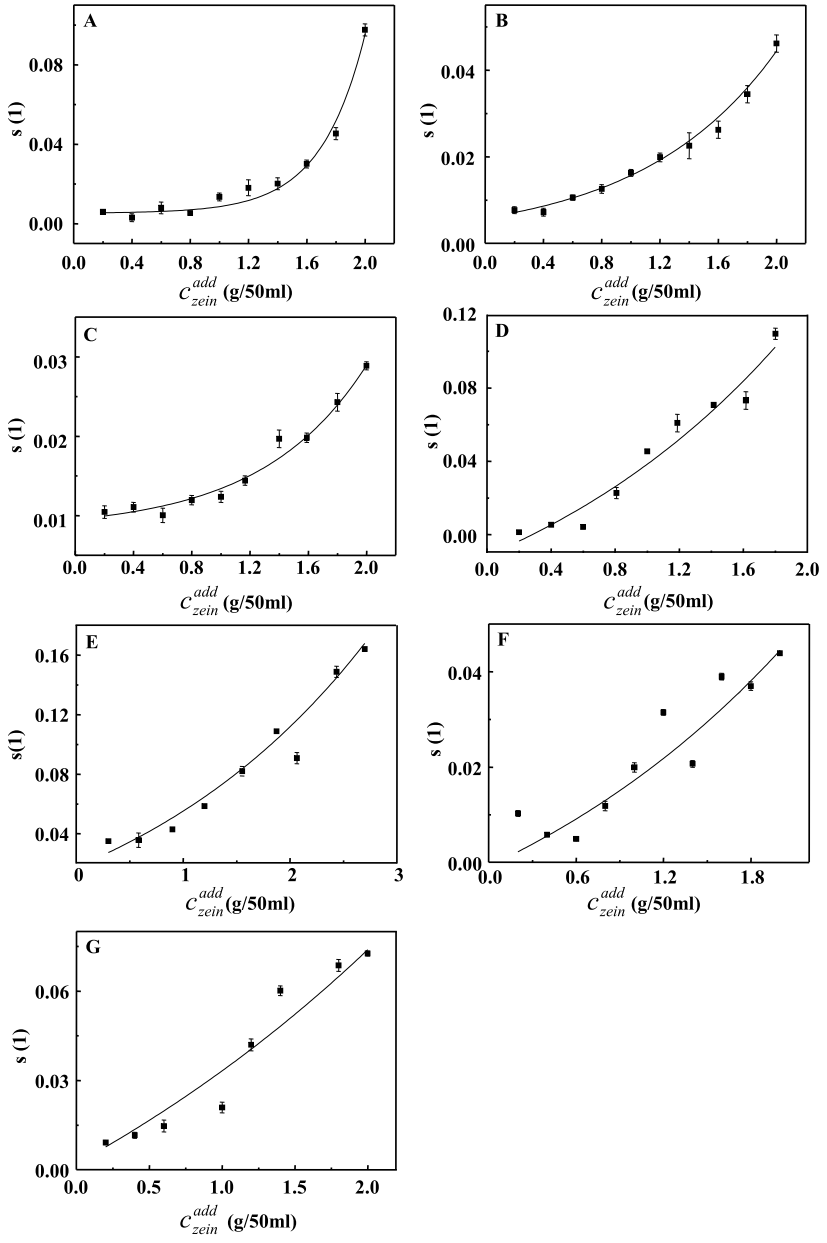

Figure 5. Relationship between s_i and c_{zein}^{add} in different Et:H_2O (w/w) solutions at 20 °C. (A) 11.4:1, (B) 10.76:1, (C) 10.1:1, (D) 9.46:1, (E) 8.8:1, (F) 8.15:1, and (G) 7.5:1.

https://doi.org/10.1021/acsomega.2c03666
ACS Omega 2022, 7, 31338−31347

and shown in Figure 6. It shows that S_{zein} decreases along with the increase of Et:H_2O ratios (w/w). Figure 6 also demonstrates

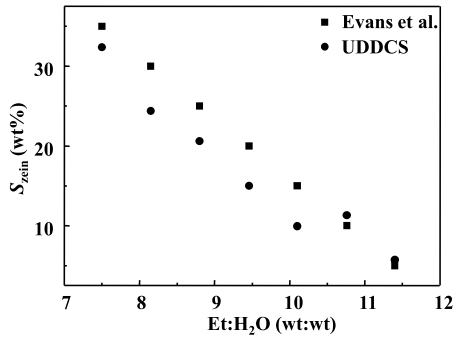

Figure 6. Comparison of zein solubility as a function of Et:H_2O (w/w) measured by Evans et al.[51] and the UDDCS method.

the comparison of zein solubility data measured by Evans et al.[51] and the UDDCS method under the same conditions; it indicates that, at low S_{zein}, the results of the two methods are consistent, but when S_{zein} increases, the data measured by the UDDCS method is smaller than that of Evans.[51]

The differences between the two solubility curves of zein under the same conditions can be explained by the principles of protein dissolution and the two methods. The principle of measuring the zein solubility in Evans et al.'s work[51] is to measure its "critical peptization temperature", that is, the temperature above which zein is soluble in all proportions and below which it is soluble only to the extent of 2% or 3%. At a low S_{zein}, if sufficient zein is added to a certain solvent system, except the dissolved zein, the undissolved part will precipitate directly rather than suspend. The solubility data measured by the two methods is the mass of the dissolved zein, and thus the solubility data are consistent. At a high S_{zein}, when sufficient zein is added to a certain solvent system, except the dissolved zein, the suspension part of zein will increase. If the zein solubility is established by measuring its "critical peptization temperature", the small crystals or aggregations in the suspension will exist steadily in the protein dispersion. However, the small crystals or aggregations in the suspension will be separated when using the UDDCS method. Therefore, at a high S_{zein}, the solubility data measured by the UDDCS method is smaller than that of Evans et al.[51]

Thus, the results of verification suggest that the UDDCS method is by no means able or meant to determine the thermodynamic solubility of a protein but determines the process-relevant stability data where the time frame allows when the metastable zone or the labile zone is reached.[48] According to the principle of protein dissolution shown in Figure 1, the protein solubility data measured by the UDDCS method would be sufficient for many applications.

In brief, it is suggested that the UDDCS method has three advantages, that is, it is reliable, universal, and time-saving. The reliable property of the UDDCS method has been verified by different methods mentioned above. The UDDCS method is a universal method based on the principle of protein dissolution because it is designed for statistics and analysis of a number of experimental results by using the constructed mathematics model. Meanwhile, the UDDCS method is a dynamic method in essence, and it does not need preparation of protein crystals and have protein solutions reach the thermodynamic equilibrium. The time consumed in each part is approximately 30 min for dispersion, 20 min for differential centrifugation, and 60 min for UV−vis measurement. The total time needed in the UDDCS method is approximately 110 min to obtain a solubility point, and thus it can evaluate the solubility curve of a certain protein within 12 h. Therefore, it is time-saving compared with other thermodynamic and dynamic methods, which need several months or weeks to obtain a solubility curve.

4.3. Results of Test Studies. *4.3.1. Effect of c_{NaOH} on Zein Solubility.* Fitted curves of s_i as a function of c_{zein}^{add} in different c_{NaOH} values at 30 °C are shown in Figure S3, and fitting parameters of a, b, and R^2 of the fitting equations are listed in Table S3. The fitting parameters are substituted into eq 2, and zein solubility data are obtained, as shown in Figure 7. It can be

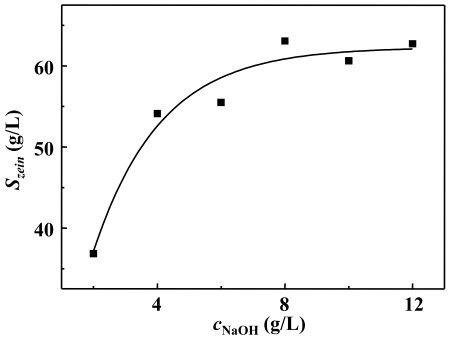

Figure 7. Solubility curve of zein solubility in different c_{NaOH} values at 20 °C.

seen that S_{zein} first increases rapidly with the increase of c_{NaOH} and reaches an upper limit. The solubility data can be well correlated as $S_{zein} = -65.35 \exp(c_{NaOH}/-2.1) + 62.3$.

The primary reason for the effect of c_{NaOH} on zein solubility in Figure 7 is analyzed as follows. Figure S4 shows the comparison between H^1 NMR spectra of zein/DMSO solution and zein/DMSO/NaOD solution. As shown in Figure S4, a large proportion of zein hydrogen bonds in DMSO disappears after adding NaOD, which demonstrates that the chemical reaction occurs. At a low c_{NaOH} (<0.15 mol/L), the structure of zein molecules is not damaged seriously, and NaOD only causes the rearrangement of hydrogen bonds, that is, reacts with −COOH in zein molecules, which increases the interaction between protein and solvents. However, at a high c_{NaOH} (>0.15 mol/L), the second and third conformation of zein molecules will be damaged, which causes structural looseness of zein molecules, and inner hydrophobic groups will be exposed.[52] Therefore, the zein solubility increases with the increase of c_{NaOH} and reaches an upper limit.

4.3.2. Effect of Temperature on Zein Solubility. Fitted curves at different temperature and fitting parameters are shown in Figure S5 and Table S4, the fitting parameters are substituted into eq 2 and zein solubility data at different temperature is obtained, as shown in Figure 8. It can be seen that S_{zein} increased first, then decreases with the increasing of temperature. The solubility data are correlated as $S_{zein} = 24.54 + \frac{4090}{\pi} \cdot \frac{14.26}{4 \times (t-29.68)^2 + 14.26^2}$, $R^2 = 0.9051$, which follows the Lorentz equation.

At a constant pH and ionic strength, the reason for the zein solubility curve first increasing and then decreasing along with the increase of temperature is analyzed as follows. The activity of protein molecules increases along with the increase of temperature from 0 to 40 °C, which makes the protein solubility

https://doi.org/10.1021/acsomega.2c03666
ACS Omega 2022, 7, 31338−31347

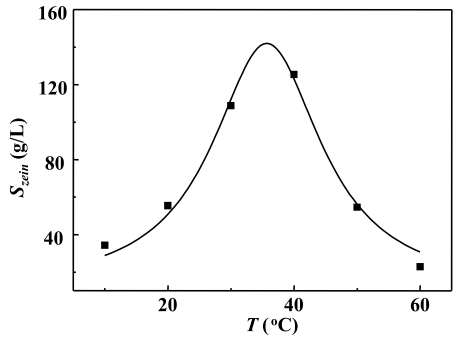

Figure 8. Solubility curve of zein solubility as a function of temperature in 6 g/L NaOH aqueous solution.

increase. When the temperature exceeds 40 °C, inner hydrophobic groups will be exposed because the kinetic energy increases and hydrogen bonds and hydration of ionic groups decrease.[53] Thus, zein molecules will aggregate and precipitate, and zein solubility decreases at >40 °C.

4.3.3. Effect of Urea on Cas Solubility. Fitted curves at different urea concentrations and fitting parameters are shown in Figure S6 and Table S5, the fitting parameters are substituted into eq 2, and Cas solubility data is obtained, as shown in Figure 9. This demonstrates that S_{Cas} decreases with the increase of c_{urea},

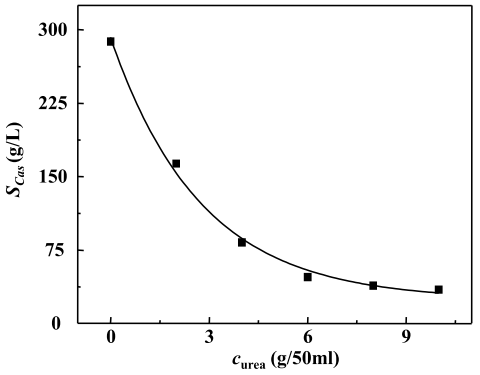

Figure 9. Solubility curve of Cas solubility as a function of c_{urea} at 25 °C.

and the possible reason is that urea decreases the hydrolyzing degree of Cas in NaOH aqueous solutions.[54] The solubility data follows the exponential equation, which is correlated as $S_{Cas} = 268.33 \exp(-c/2.76) + 24.01$, $R^2 = 0.9915$.

5. CONCLUSIONS

In summary, the developed UDDCS method, which is based on the principle of protein dissolution, includes the following steps: (1) the protein is thoroughly dispersed into a certain solvent using ultrasonics and stirring and then quickly reaches the dissolution equilibrium; (2) the stability of the dispersion system is evaluated using the differential centrifugation technique; (3) the concentration of the centrifugate at different centrifugal speeds is tested using a UV−vis spectrometer; (4) the s_i of the centrifugate concentration is calculated; (5) when protein dispersion systems with different added concentrations are treated by the steps mentioned above, a modified exponential equation is selected to correlate the relationship between s_i and c_i^{add}; and (6) the curvature equation of the modified exponential equation is calculated, and the corresponding concentration of the maximum curvature value, which means the fastest deterioration of the stability for a protein dispersion system, is determined as the solubility of protein.

The verification results of Ly solubility in NaCl aqueous solutions indicate that the "solubility curve" measured by the UDDCS method is basically the ML curve, which completely accords with the original design of the UDDCS method. The verification results of zein solubility in Et aqueous solution also confirm the reliability of the UDDCS method.

The UDDCS method is successfully applied to evaluate zein solubility in NaOH solution and Cas solubility in urea aqueous solutions. The total time needed in the UDDCS method is approximately 110 min to obtain a solubility point, and it can evaluate the solubility curve of a certain protein within 12 h. Thus, the UDDCS method is suitable for fast and reliable assessment of protein solubility.

■ ASSOCIATED CONTENT

Supporting Information

The Supporting Information is available free of charge at https://pubs.acs.org/doi/10.1021/acsomega.2c03666.

Equations of protein added concentrations, standard curve equations of proteins in solvents, standard deviation, curvature equation, and first derivative of the curvature equation, c_i^{add}, eqs S2, S3, S4, and S5, s_i, K, and K'; effects of ultrasonic and centrifugal time on protein dispersion, s_i as a function of c_{zein}^{add} and c_{Cas}^{add}, H^1 NMR spectra of zein in deuterated DMSO solution and deuterated DMSO/NaOD solution; and fitting parameters of a, b, and R^2 in Figures 3 and 5 and Figures S3, S5, and S6 (PDF)

■ AUTHOR INFORMATION

Corresponding Authors

Jun Fang − *School of Chemical Engineering and Materials Science, Quanzhou Normal University, Quanzhou 362000, China;* orcid.org/0000-0001-5152-5497; Email: fangjun@qztc.edu.cn

Yanbin Jiang − *School of Chemistry and Chemical Engineering, South China University of Technology, Guangzhou 510640, China;* orcid.org/0000-0001-8984-0302; Email: cebjiang@scut.edu.cn

Authors

Dongwei Wei − *School of Chemical Engineering and Materials Science, Quanzhou Normal University, Quanzhou 362000, China*

Meng Wang − *School of Chemical Engineering and Materials Science, Quanzhou Normal University, Quanzhou 362000, China*

Hongdi Wang − *College of Material, Chemistry and Chemical Engineering, Key Laboratory of Organosilicon Chemistry and Material Technology, Ministry of Education, Hangzhou Normal University, Hangzhou 311121 Zhejiang, China*

Guijin Liu − *School of Pharmaceutical Sciences, Hainan University, Haikou 570228, China;* orcid.org/0000-0002-2175-3154

Complete contact information is available at: https://pubs.acs.org/10.1021/acsomega.2c03666

Notes

The authors declare no competing financial interest.

https://doi.org/10.1021/acsomega.2c03666
ACS Omega 2022, 7, 31338−31347

■ ACKNOWLEDGMENTS

D.W. and M.W. received funding from the Natural Science Foundation of Fujian Province (no. 2019J01731), Young and Middle-Aged Teacher Education Scientific Research Project of Fujian Province (no. JT180368), and Startup Fund for Talents of Quanzhou Normal University (no. H18020). H.W. received funding from the Natural Science Foundation of Zhejiang Province (no. LQ20B060003). G.L. received funding from the Natural Science Foundation of Hainan Province (no. 820QN249) and National Natural Science Foundation of China (no. 22008046). J.F. received funding from the National Natural Science Foundation of China (nos. 21676222 and U1705252). Y.J. received funding from the National Natural Science Foundation of China (no. 22178121).

■ ABBREVIATION

a, b = fitting parameters of equations (−)
A = absorbance (1)
c_{Cas} = concentration of Cas (g/L)
c_i^{add} = protein concentration originally added (g/L)
$c_i^{j_n}$ = protein concentration after differential centrifugation (g/L)
$\bar{c}_i^{j_n}$ = average value of the protein concentration after differential centrifugation (g/L)
c_{Ly}^{add} = concentration of Ly originally added (g/L)
c_{NaCl} = concentration of NaCl (g/L)
c_{NaOH} = concentration of NaOH (g/L)
$c_{protein}$ = concentration of the protein (g/L)
c_{zein} = concentration of zein originally added (g/L)
i = number of protein samples (−)
j_n = centrifugal speeds (rpm)
K = curvature (−)
K' = first derivative (−)
m_i = mass of protein added (g)
n = number of centrifugal tubes (−)
rpm = revolutions per minute
R^2 = correlation index (−)
s_i = standard deviation values (−)
s_i' = first derivative of s_i (−)
s_i'' = second derivative of s_i (−)
S = protein solubility (g/L)
S_{Cas} = Cas solubility (g/L)
S_{Ly} = Ly solubility (g/L)
S_{zein} = zein solubility (g/L)
t_c = centrifugal time (min)
t_u = ultrasonic time (s)
T = temperature (°C)
λ = characteristic absorbance peak (nm)

■ REFERENCES

(1) Dekker, M.; Riet, K. V.; Bijsterbosch, B. H.; Fijneman, P.; Hilhorst, R. Mass transfer rate of protein extraction with reversed micelles. *Chem. Eng. Sci.* **1990**, *45*, 2949−2957.
(2) Curtis, R. A.; Lue, L. A molecular approach to bioseparations: protein−protein and protein−salt interactions. *Chem. Eng. Sci.* **2006**, *61*, 907−923.
(3) Trevino, S. R.; Scholtz, J. M.; Pace, C. N. Measuring and increasing protein solubility. *J. Pharm. Sci.* **2008**, *97*, 4155−4166.
(4) Kwon, J. S. I.; Nayhouse, M.; Orkoulas, G.; Ni, D.; Christofides, P. D. Run-to-Run-Based Model Predictive Control of Protein Crystal Shape in Batch Crystallization. *Ind. Eng. Chem. Res.* **2015**, *54*, 4293−4302.
(5) Kwon, J. S. I.; Nayhouse, M.; Orkoulas, G.; Christofides, P. D. Enhancing the Crystal Production Rate and Reducing Polydispersity in Continuous Protein Crystallization. *Ind. Eng. Chem. Res.* **2014**, *53*, 15538−15548.
(6) Kwon, J. S.-I.; Nayhouse, M.; Christofides, P. D.; Orkoulas, G. Protein crystal shape and size control in batch crystallization: Comparing model predictive control with conventional operating policies. *Ind. Eng. Chem. Res.* **2014**, *53*, 5002−5014.
(7) Thommes, J.; Etzel, M. Alternatives to chromatographic separations. *Biotechnol. Prog.* **2007**, *23*, 42−45.
(8) Low, D.; O'Leary, R.; Pujar, N. S. Future of antibody purification. *J. Chromatogr. B* **2007**, *848*, 48−63.
(9) Gagnon, P.; Mayes, T.; Danielsson, A. An adaptation of hydrophobic interaction chromatography for estimation of protein solubility optima. *J. Pharm. Biomed. Anal.* **1997**, *16*, 587−592.
(10) To, B. C. S.; Lenhoff, A. M. Hydrophobic interaction chromatography of proteins II. Solution thermodynamic properties as a determinant of retention. *J. Chromatogr. A* **2007**, *1141*, 235−243.
(11) Aghanouri, A.; Shoemaker, C. F.; Sun, G. Characterization of Conformational Structures of Plant Proteins in Solutions. *Ind. Eng. Chem. Res.* **2015**, *54*, 188−197.
(12) Hachem, F.; Andrews, B. A.; Asenjo, J. A. Hydrophobic partitioning of proteins in aqueous two-phase systems. *Enzyme Microb. Technol.* **1996**, *19*, 507−517.
(13) Black, S. N.; Collier, E. A.; Davey, R. J.; Roberts, R. J. Structure, solubility, screening, and synthesis of molecular salts. *J. Pharm. Sci.* **2007**, *96*, 1053−1068.
(14) Martins, I. M.; Barreiro, M. F.; Coelho, M.; Rodrigues, A. E. Microencapsulation of essential oils with biodegradable polymeric carriers for cosmetic applications. *Chem. Eng. J.* **2014**, *245*, 191−200.
(15) Lü, S.; Liu, M.; Ni, B. Degradable, injectable poly(N-isopropylacrylamide)-based hydrogels with low gelation concentrations for protein delivery application. *Chem. Eng. J.* **2011**, *173*, 241−250.
(16) Dale, G. E.; Oefner, C.; D'Arcy, A. The protein as a variable in protein crystallization. *J. Struct. Biol.* **2003**, *142*, 88−97.
(17) Mitra, K.; Steitz, T. A.; Engelman, D. M. Rational design of "water-soluble" bacteriorhodopsin variants. *Protein Eng.* **2002**, *15*, 485−492.
(18) Evans, P.; Wyatt, K.; Wistow, G. J.; Bateman, O. A.; Wallace, B. A.; Slingsby, C. The P23T cataract mutation causes loss of solubility of folded γ D-crystallin. *J. Mol. Biol.* **2004**, *343*, 435−444.
(19) Kirk, O.; Borchert, T. V.; Fuglsang, C. C. Industrial enzyme applications. *Curr. Opin. Biotechnol.* **2002**, *13*, 345−351.
(20) Carpenter, J. F.; Kendrick, B. S.; Chang, B. S.; Manning, M. C.; Randolph, T. W. Inhibition of stress-induced aggregation of protein therapeutics. *Methods Enzymol.* **1999**, *309*, 236−255.
(21) Wang, W. Instability, stabilization, and formulation of liquid protein pharmaceuticals. *Int. J. Pharm.* **1999**, *185*, 129−188.
(22) Pusey, M. L.; Gernert, K. A method for rapid liquid-solid phase solubility measurements using the protein lysozyme. *J. Cryst. Growth* **1988**, *88*, 419−424.
(23) Lu, J.; Wang, X. J.; Ching, C. B. Batch crystallization of soluble proteins: effect of precipitant, temperature and additive. *Prog. Cryst. Growth Charact. Mater.* **2002**, *45*, 201−217.
(24) Howard, S. B.; Twigg, P. J.; Baird, J. K.; Meehan, E. J. The solubility of hen egg-white lysozyme. *J. Cryst. Growth* **1988**, *90*, 94−104.
(25) Ducruix, A. F.; Ries-Kautt, M. M. Solubility diagram analysis and the relative effectiveness of different ions on protein crystal growth. *Methods* **1990**, *1*, 25−30.
(26) Asherie, N. Protein crystallization and phase diagrams. *Methods* **2004**, *34*, 266−272.
(27) Benvenuti, M.; Mangani, S. Crystallization of soluble proteins in vapor diffusion for X-ray crystallography. *Nat. Protoc.* **2007**, *2*, 1633−1651.
(28) Cacioppo, E.; Munson, S.; Pusey, M. L. Protein solubilities determined by a rapid technique and modification of that technique to a micro-method. *J. Cryst. Growth* **1991**, *110*, 66−71.

https://doi.org/10.1021/acsomega.2c03666
ACS Omega 2022, 7, 31338−31347

(29) Pusey, M. L.; Gernert, K. A method for rapid-solid-phase solubility measurement using the protein lysozyme. *J. Cryst. Growth* **1988**, *88*, 419−424.
(30) Pusey, M. L.; Munson, S. Micro-apparatus for rapid determinations of protein solubilities. *J. Cryst. Growth* **1991**, *113*, 385−389.
(31) Suzuki, Y.; Sazaki, G.; Visuri, K.; Tamura, K.; Nakajima, K.; Yanagiya, S.-i. Significant decrease in the solubility of glucose isomerase crystals under high pressure. *Cryst. Growth Des.* **2002**, *2*, 321−324.
(32) Rosenberger, F.; Howard, S. B.; Sowers, J. W.; Nyce, T. A. Temperature dependence of protein solubility-determination and application to crystallization in X-ray capillaries. *J. Cryst. Growth* **1993**, *129*, 1−12.
(33) Feeling-Taylor, A. R.; Banish, R. M.; Elison Hirsch, R.; Vekilov, P. G. Miniaturized scintillation technique for protein solubility determinations. *Rev. Sci. Instrum.* **1999**, *70*, 2845−2849.
(34) Sazaki, G.; Kurihara, K.; Nakada, T.; Miyashita, S.; Komatsu, H. A novel approach to the solubility measurement of protein crystals by two-beam interferometry. *J. Cryst. Growth* **1996**, *169*, 355−360.
(35) Gray, R. J.; Hou, W. B.; Kudryavtsev, A. B.; Delucas, L. J. A new approach to the measurement of protein solubility by Michaelson interferometry. *J. Cryst. Growth* **2001**, *232*, 10−16.
(36) Nakazato, K.; Homma, T.; Tomo, T. Rapid solubility measurement of protein crystals as a function of precipitant concentration with micro-dialysis cell and two-beam interferometer. *J. Synchroton Radiat.* **2004**, *11*, 34−37.
(37) Van Driessche, A. E. S.; Gavira, J. A.; Patiño Lopez, L. D.; Otalora, F. Precise Protein Solubility Determination by Laser Confocal Differential Interference Contrast Microscopy. *J. Cryst. Growth* **2009**, *311*, 3479−3484.
(38) Mata, J. P.; Udabage, P.; Gilbert, E. P. Structure of casein micelles in milk protein concentrate powders via small angle X-ray scattering. *Soft Matter* **2011**, *7*, 3837−3843.
(39) Haire, L. F.; Blow, D. M. A novel spin filter method for the measurement of solubility. *J. Cryst. Growth* **2001**, *232*, 17−20.
(40) Maosoongnern, S.; Diaz Borbon, V.; Flood, A. E.; Ulrich, J. Introducing a fast method to determine the solubility and metastable zone width for proteins: case study lysozyme. *Ind. Eng. Chem. Res.* **2012**, *51*, 15251−15257.
(41) Tomlinson, S. R.; Kehr, C. W.; Lopez, M. S.; Schlup, J. R.; Anthony, J. L. Solubility of the corn protein zein in imidazolium-based ionic liquids. *Ind. Eng. Chem. Res.* **2014**, *53*, 2293−2298.
(42) Ataka, M.; Asai, M. Systematic studies on the crystallization of lysozyme. Determination and use of phrase diagrams. *J. Cryst. Growth* **1988**, *90*, 86−93.
(43) Berg, A.; Schuetz, M.; Dismer, F.; Hubbuch, J. Automated measurement of apparent protein solubility to rapidly assess complex parameter interactions. *Food Bioprod. Process.* **2014**, *92*, 133−142.
(44) Chen, T. M.; Shen, H.; Zhu, C. Y. Evaluation of a method for high throughput solubility determination using a multi-wavelength UV plate reader. *Comb. Chem. High Throughput Screening* **2002**, *5*, 575−581.
(45) Pan, L.; Ho, Q.; Tsutsui, K.; Takahashi, L. Comparison of chromatographic and spectroscopic methods used to rank compounds for aqueous solubility. *J. Pharm. Sci.* **2001**, *90*, 521−529.
(46) van Oss, C. J.; Good, R. J.; Chaudhury, M. K. Solubility of Proteins. *J. Protein Chem.* **1986**, *5*, 385−405.
(47) Li, Y.; Li, J.; Xia, Q.; Zhang, B.; Wang, Q.; Huang, Q. Understanding the dissolution of α-zein in aqueous ethanol and acetic acid solutions. *J. Phys. Chem. B* **2012**, *116*, 12057−12064.
(48) Wiendahl, M.; Völker, C.; Husemann, I.; Krarup, J.; Staby, A.; Scholl, S.; Hubbuch, J. A novel method to evaluate protein solubility using a high throughput screening approach. *Chem. Eng. Sci.* **2009**, *64*, 3778−3788.
(49) Thomas, G. B.; Weir, M. D.; Hass, J.; Giodano, F. R. *Thomas Calculus. Pearson Education*, 11th Edition, 2004: pp. 936−943.
(50) Forsythe, E. L.; Judge, R. A.; Pusey, M. L. Tetragonal chicken egg white lysozyme solubility in sodium chloride solutions. *J. Chem. Eng. Data* **1999**, *44*, 637−640.
(51) Evans, C. D.; Manley, R. H. Ternary solvents for zein. *Ind. Eng. Chem.* **1944**, *36*, 408−410.
(52) Law, A. J.; Leaver, J. Effect of pH on the thermal denaturation of whey proteins in milk. *J. Agric. Food Chem.* **2000**, *48*, 672−679.
(53) Rüegg, M.; Moor, U.; Blanc, B. A calorimetric study of the thermal denaturation of whey proteins in simulated milk ultrafiltrate. *J. Dairy Res.* **1977**, *44*, 509−520.
(54) McGann, T. C. A.; Fox, P. F. Physico-chemical properties of casein micelles reformed from urea-treated milk. *J. Dairy Res.* **1974**, *41*, 45−53.

https://doi.org/10.1021/acsomega.2c03666
ACS Omega 2022, 7, 31338−31347